JOC Article

Dual Binding Mode of Methylmethanetriacetic Acid to Tripodal Amidopyridine Receptors

Pablo Ballester,*,† Magdalena Capó,† Antoni Costa,† Pere M. Deyà,† Rosa Gomila,† Andreas Decken,‡ and Ghislain Deslongchamps‡

Departament de Química, Universitat de les Illes Balears, 07071 Palma de Mallorca, Spain, and Department of Chemistry, University of New Brunswick, Fredericton, New Brunswick, E3B 6E2, Canada

pablo.ballester@uib.es

Received April 2, 2002

A series of tripodal amidopyridine receptors capable of selective recognition of methylmethanetriacetic acid (MMTA) in organic solvents is described. Intramolecular hydrogen-bonding groups, built into some of the receptors, were designed as preorganization devices. Binding was studied by NMR titration, variable temperature NMR experiments, 2D-NMR, isothermal titration calorimetry, and single-crystal X-ray crystallography. The results reveal that a balancing act between inter- and intramolecular hydrogen-bonding interactions in the complexes governs both the dynamics and the geometry of binding. Receptor **1b** (without intramolecular hydrogen-bonding groups) features a simple symmetric MMTA binding geometry with optimal enthalpic interactions. In sharp contrast, receptor **1a** (with intramolecular hydrogen-bonding groups) reveals a temperature-dependent dual binding mode where MMTA can bind in two completely different geometries. The two solution binding geometries of **1a**·**MMTA** were unraveled by NMR experiments and correlated to the X-ray structures.

Introduction

Intermolecular interactions are the fundamental basis for the formation of supermolecules.[1] They occur between atoms that are not directly linked by a covalent framework. In nonpolar organic solvents, the so-called "strong" or "conventional" hydrogen bond[2] (O,N)−H···(O,N), an electrostatic force with some covalent character, is probably the most important directional intermolecular force used for supramolecular construction. The design of abiotic receptors possessing high affinity and selectivity and based primarily on complementary intermolecular hydrogen-bonding arrays depends wholly on the optimization of these intermolecular interactions. This is typically achieved by tailoring the host molecular structure to that of the guest.[3] While the broad features of the supermolecule structure may be appreciated by simple consideration of optimal intermolecular hydrogen-bonding interactions and their anisotropic properties, an in-depth understanding of the design may require a detailed accounting of the interplay between inter- and intramolecular forces.[4]

In particular, we have been interested in the effect of remote intramolecular hydrogen bonding, used as a receptor preorganization device, on the detailed thermodynamics of binding and on the geometry of the complex. Initial studies focused on the molecular recognition of *cis*-1,3,5-cyclohexanetricarboxylic acid (CTA) **2** by triamidopyridine receptors **1a** and **1b**, in which the three interaction units are separated by a 1,3,5-triarylbenzene molecular scaffold. Receptor **1a** features one intramolecular hydrogen bond between the phenolic hydrogen and the amide carbonyl on each arm, restricting the receptor conformation and flexibility. These interactions were eliminated in receptor **1b** by removing the hydroxyl groups.

The structural modifications are remote with respect to the binding site and do not seem likely to affect the binding properties of the receptor due to enthalpic,[5] steric, or solvation effects.

On one hand, our binding studies on receptors **1a** and **1b** with CTA indicate that only one of two possible binding geometries is observed in solution[6,7] and in the crystalline state.[7,8] The preferred geometry for the bound

* To whom correspondence should be addressed. Current address: The Skaggs Institute for Chemical Biology, The Scripps Research Institute, MB-26, 10550 North Torrey Pines Road, La Jolla, CA 92037, on sabbatical leave from UIB. E-mail: pauba@scripps.edu.

† Universitat de les Illes Balears.

‡ University of New Brunswick.

(1) Atwood, J. L.; Davies, J. E. D.; Macnicol, D. D.; Vötgle, F., Eds. *Comprehensive Supramolecular Chemistry*; Pergamon: 1996.

(2) Jeffrey, G. A. *An Introduction to Hydrogen Bonding*; Oxford University Press: New York, 1997.

(3) Examples of abiotic receptors based on hydrogen bonding: (a) Hamilton, A. D.; Springer-Verlag: Berlin, 1991; Vol. 2, pp 115−174. (b) Rebek, J., Jr. *Angew. Chem., Int. Ed. Engl.* **1990**, *29*, 245−255. (c) Webb, T. H.; Wilcox, C. S. *Chem. Soc. Rev.* **1993**, *22*, 383−395. (d) Bell, T. W.; Hext, N. M.; Khasanov, A. B. *Pure Appl. Chem.* **1998**, *70*, 2371−2377.

(4) (a) Adams, H.; Carver, F. J.; Hunter, C. A.; Osborne, N. J. *Chem. Commun.* **1996**, 2529−2530. (b) Rebek, J., Jr.; Williams, K.; Parris, K.; Ballester, P.; Jeong, K.-S. *Angew. Chem., Int. Ed. Engl.* **1987**, *26*, 1244−1245. (c) Muehldorf, A. V.; Vanengen, D.; Warner, J. C.; Hamilton, A. D. *J. Am. Chem. Soc.* **1988**, *110*, 6561−6562. (d) Low, J. N.; Storey, E. J.; McCarron, M.; Wardell, J. L.; Ferguson, G.; Glidewell, C. *Acta Crystallogr.* **2000**, *B56*, 58−67.

(5) Rebek, J., Jr. *Acc. Chem. Res.* **1990**, *23*, 399−404.

(6) Ballester, P.; Costa, A.; Deyà, P. M.; Gonzalez, J. F.; Rotger, M. C. *Tetrahedron Lett.* **1994**, *35*, 3813−3816.

10.1021/jo0257871 CCC: $22.00
Published on Web 11/16/2002

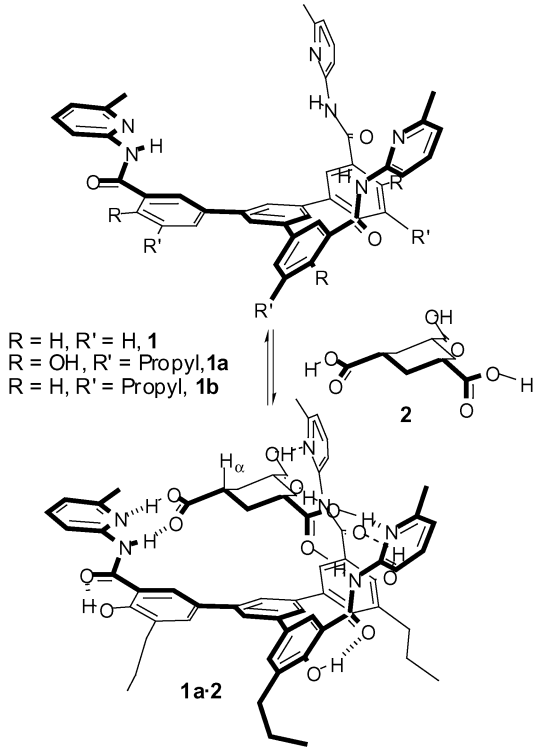

FIGURE 1. Preferred binding geometry of **1a** or **1b** and **2**.

guest features the three axial hydrogens α to the carboxyl groups pointing outside the receptor cavity (Figure 1, H_α). On the other hand, receptor **1b**, which lacks the intramolecular hydrogen bonds, exhibits an enthalpy for binding CTA that is ~ 3 kcal/mol higher than that measured for intramolecularly hydrogen-bonded receptor **1a**. On the basis of Koshland's induced-fit hypothesis,[9] the optimum host conformation for binding CTA could be inferred from the X-ray complex structure for **1b·2**,[7] which reveals an average value of 23° (0.97) for the dihedral angle between the carboxamide and aryl planes. In contrast, that same dihedral angle is only 10° (2.3) for the **1a·2**[8] complex. Thus, host **1a** cannot achieve the optimum binding conformation due to conformational restrictions imposed by the intramolecular phenolic hydrogen bonds. We concluded that the preferred binding geometry was derived from a maximization of the intermolecular interactions, while the difference in the enthalpy of binding was a consequence of a balance between the inter- and intramolecular hydrogen-bonding interactions.

Herein we report a complementary study focused on the molecular recognition of methylmethanetriacetic acid (MMTA, 3-carboxymethyl-3-methylpentanedioic acid, **3**) by receptors **1a** and **1b**, complete with full experimental details of the receptor syntheses.

In the case of MMTA recognition, the balancing of inter- and intramolecular hydrogen-bonding interactions was not only reflected in a difference of binding enthalpies toward receptors **1a** and **1b** but also in totally different binding behaviors. Indeed, while receptor **1a** binds MMTA in a single geometry, receptor **1b** features a dual binding mode. The dynamic process in which complex **1b·3** is involved was studied by variable temperature (VT) ^{1}H NMR spectroscopy. As will be apparent from the following section, at low temperature, the favored binding geometry results from a maximization of intermolecular interactions, while at room temperature it is the maximization of intramolecular interactions that appears to govern the preferred geometry. Thus, the relative distribution of the geometric complexes for **1b·3** is controlled by the interplay of inter- and intramolecular interactions, which in turn is regulated by temperature.

Results and Discussion

Design and Synthesis. Some time ago, some of us reported[10] the use of a tetrachlorosilane−ethanol-induced self-condensation of ketones[11] for preparing 1,3,5-tris(3-bromo-4-hydroxy-5-carboxyphenyl)benzene. With this facile synthetic methodology, one can obtain 1,3,5-triaryl-substituted benzenes in multigram quantities. Molecular modeling studies[12] on the corresponding debrominated 2-amidopyridine derivative **1** suggested that the syn conformation of the molecule was very well suited for the complexation of CTA **2** (Figure 1) and MMTA **3** (Figure 4). In this conformation, the hydrogen-bonding groups converge and act simultaneously in "grasping" the guest molecule in the induced cleft of the receptor. It is worth noting that, in the original design of the host, intramolecular hydrogen bonding between the amide carbonyls and the phenol protons was intended simply as a preorganization tool.[13] The other possible conformer, in which the amide protons are hydrogen-bonded to the phenolic oxygens, was dismissed on thermodynamic grounds.[14] Thus, the favored intramolecular hydrogen bonds restrict the rotation of the $C_{aryl}-C_{amide}$ single bonds, forcing the amide hydrogens to point toward the interior of the cavity, locking each binding subunit in a conformation that is quasiplanar with each aryl ring. The evaluation of the goodness of the designed intramolecular hydrogen bonds as a preorganization tool required the synthesis of the analogous deoxygenated receptor **1b**.

The synthesis of host **1** was straightforward and is outlined in Scheme 1. Receptor **1** was prepared from triester **5**, which was obtained in 78% yield through tetrachlorosilane−ethanol-induced self-condensation of 4-acetylmethylsalicylate[15] **4**. Next, the phenol hydroxyls of triester **5** were protected as benzyl ethers to afford the tribenzylated triester **6**,[14] a step that was found necessary in order to cleanly obtain the triacyl chloride in a later step. The tribenzylated triester was hydrolyzed under

(7) Ballester, P.; Capó, M.; Costa, A.; Deyà, P. M.; Gomila, R.; Decken, A.; Deslongchamps, G. *Org. Lett.* **2001**, *3*, 267−270.
(8) Ballester, P.; Costa, A.; Deyà, P. M.; Deslongchamps, G.; Mink, D.; Decken, A.; Prohens, R.; Tomàs, S.; Vega, M. *J. Chem. Soc., Chem. Commun.* **1997**, 357−358.
(9) Koshland, D. E. *Proc. Natl. Acad. Sci.* **1958**, *44*, 98.
(10) Rotger, M. C.; Costa, A.; Saá, J. M. *J. Org. Chem.* **1993**, *58*, 4083−4087.
(11) Elmorsy, S. S.; Pelter, A.; Smith, K.; Hursthouse, M. B.; Ando, D. *Tetrahedron Lett.* **1992**, *33*, 821−824.
(12) Macromodel V6.0: Mohamadi, F.; Richards, N. G. J.; Guida, W. C.; Liskamp, R.; Lipton, M.; Caulfield, C.; Chang, G.; Hendrickson, T.; Still, W. C. *J. Comput. Chem.* **1990**, *11*, 440.
(13) (a) Cram, D. J. *Angew. Chem., Int. Ed. Engl.* **1986**, *25*, 1039−1058. Examples of conformational restriction by intramolecular hydrogen bonding: (b) López de la Paz, M.; Ellis, G.; Penadés, S.; Vicent, C. *Tetrahedron Lett.* **1997**, *38*, 1659−1662. (c) Kohmoto, S.; Koyano, I.; Kawatsuji, T.; Kasimura, H.; Kishikawa, K.; Yamamoto, M.; Yamada, K. *Bull. Chem. Soc. Jpn.* **1996**, *69*, 3261−3265.
(14) Garrett, T. M.; Cass, M. E.; Raymond, K. N. *J. Coord. Chem.* **1992**, *25*, 241−253.

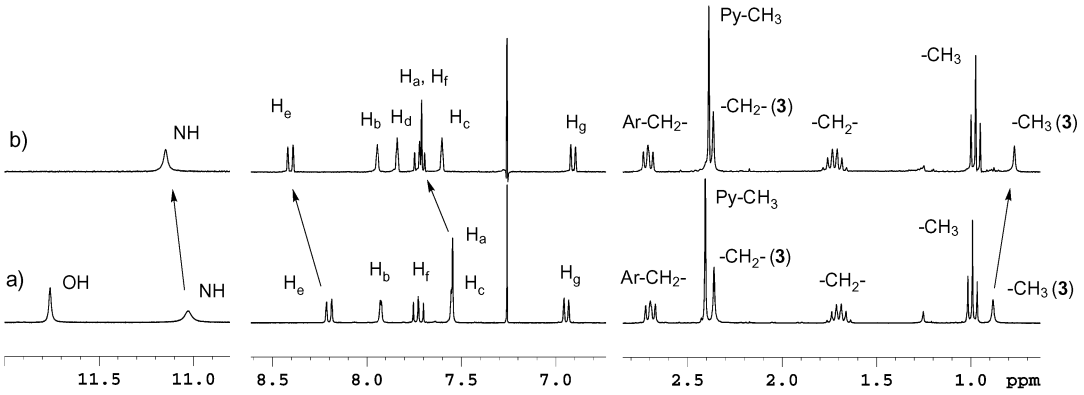

FIGURE 2. ^{1}H NMR spectra of complexes (a) **1a·3** and (b) **1b·3** in $CDCl_3$ at 298 K. See Figure 4 for protons assignments.

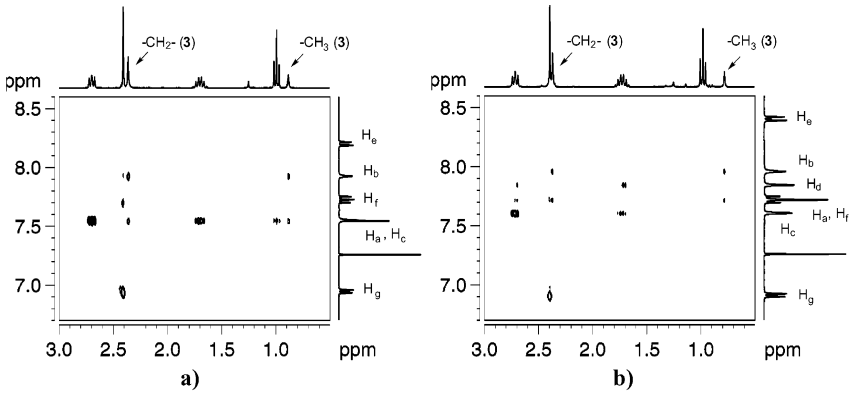

FIGURE 3. Expanded regions of the 2D-ROESY spectra of (a) complex **1a·3** and (b) complex **1b·3** in $CDCl_3$ at 298 K.

basic conditions to afford, after acidification, the tribenzylated triacid **7** in 96% yield. Triacid **7** was converted almost quantitatively to the corresponding triacid chloride **8** by treatment with thionyl chloride. Next, the triacid chloride **8** was coupled with 2-amino-6-methylpyridine, yielding triamide **9**. Finally, the benzyl groups were removed using TMSI or HBr, affording receptor **1** (38% overall yield from **4**, Scheme 1) as a white solid, insoluble in $CHCl_3$ or other organic solvents that cannot disrupt hydrogen bonding.

To increase the chloroform solubility of the receptor, a more lipophilic version of the triaryl spacer was devised. The synthesis involved the etherification of the phenols of **5** with allyl bromide[16] to obtain compound **10**, followed by a triple Claisen[17] rearrangement, yielding **11**, and finally catalytic hydrogenation of the terminal double bonds to afford the propylated triaryl benzene triester **5a** in 61% overall yield (Scheme 2).

Receptors **1a** and **1b** were prepared uneventfully using lipophilic spacer **5a**. For the preparation of **1a**, a benzene solution of **5a** (previously treated with 1.5 equiv of trimethylaluminum) was refluxed with 1.5 equiv of the trimethylaluminum complex of 2-aminopicoline for 48 h,[18] resulting in a 26% yield of host **1a** after column chromatography (Scheme 2). Chloroform solutions of receptor **1a** of up to 10^{-2} M could be easily prepared.

Host **1b** was also prepared from triester **5a** through a more elaborated route. First, the phenols of **5a** were removed by converting triester **5a** to the corresponding tris aryl triflate **12**, followed by ring deoxygenation mediated by $Cl_2Pd(PPh_3)_2$[19] to afford triester **5b** in 63% overall yield. Hydrolysis of triester **5b** afforded triacid **14**, which was converted to the triacyl chloride **15** on treatment with thionyl chloride. Finally, **15** was coupled with 6-methyl-2-aminopyridine to produce tripodal receptor **1b** (38% overall yield, from **5a**, Scheme 2). Receptor **1b** was also quite soluble in chloroform.

Binding Studies. Addition of solid MMTA **3** to a room-temperature $CDCl_3$ solution of either receptor **1a** or **1b** led to rapid dissolution of the otherwise insoluble substrate. In both cases, large downfield shifts (~3 ppm) were observed for the NH resonances, indicating the formation of hydrogen-bonded complexes, which integration established as having 1:1 stoichiometry. Dilution of a 5 mM $CDCl_3$ solution of each pair of components to 0.5 mM shows negligible changes in the chemical shifts, suggesting a $K_a > 1 \times 10^4$ M^{-1} for hosts **1a** and **1b** with triacid **3** in chloroform.

(15) Originally the triester **1b** was prepared through the tetrachlorosilane−ethanol-induced self-condensation of 4-acetylsalicylic acid (see ref 10), followed by esterification with diazomethane. In the course of this work, we found that when the self-condensation reaction is carried out on 4-acetylmethylsalicylate, the triester **1b** is obtained in just one synthetic step in a higher yield and with a simpler workup.

(16) Winters, R. T.; Sercel, A. D.; Showalter, H. D. H. *Synthesis* **1988**, 712−714.

(17) Danishefsky, S.; Berman, E. M.; Ciufolini, M.; Etheredge, S. J.; Segmuller, B. E. *J. Am. Chem. Soc.* **1985**, *107*, 3891−3898.

(18) Basha, A.; Lipton, M.; Weinreb, S. M. *Tetrahedron Lett.* **1977**, 4171−4173.

(19) (a) Saá, J. M.; Dopico, M.; Martorell, G.; García-Raso, A. *J. Org. Chem.* **1990**, *55*, 991−995. (b) Cacchi, S.; Ciattini, P. G.; Morera, E.; Ortar, G. *Tetrahedron Lett.* **1986**, *27*, 5541−5544.

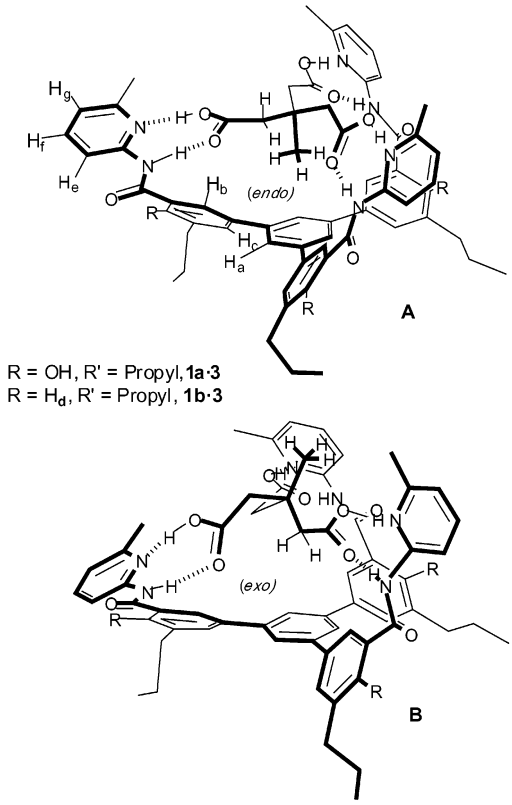

FIGURE 4. Possible binding geometries for 1:1 complexes **1a·3** and **1b·3**. The terms endo and exo refer to the orientation of the methyl group of **3** with respect to the receptor cavity.

The ^{1}H NMR spectra for the complexes **1a·3** and **1b·3** are shown in Figure 2. Similar chemical shifts are observed for several of the equivalent protons in the two different complexes, such as, the propyl chain protons and some of the aromatic and aliphatic resonances. However, the ^{1}H NMR spectrum of complex **1b·3** (Figure 2b) shows a significant downfield shift for the singlet assigned to the central aromatic ring protons (H_a), one of the pyridine doublets (H_e), and the amide NH signal when compared to complex **1a·3**. Also, a moderate upfield shift is observed for the methyl singlet of triacid **3** in complex **1b·3** compared to the same signal for complex **1a·3**. As a whole, these observations lead one to surmise that a different binding mode for each of the complexes was operative. To explore this hypothesis, 2D-ROESY[20] spectra (mixing time = 500 ms, spinlock = 2 kHz) were acquired at room temperature for each of the complexes (Figure 3).

Figure 3a shows an expansion of the 2D-ROESY spectrum obtained for complex **1a·3**. Intermolecular contacts between the protons of the receptor and the triacid were observed. Indeed, correlation peaks between the methyl and methylene signals of MMTA and the H_a and H_b protons of the receptor are clearly evident. The 2D-ROESY for complex **1b·3** (Figure 3b) is identical in terms of observed cross-peaks. A difference arises when the ratio of integral volumes for the above-mentioned cross-peaks is calculated. For complex **1a·3**, the ratio of integrals for the cross-peaks between the H_a proton of the receptor and the methyl and methylene triacid signals was 0.79 (cross-peak volume CH_3(**3**)$-H_a$/cross-peak volume CH_2(**3**)$-H_a$). The corresponding ratio for the H_b proton was 0.53. Similarly, for complex **1b·3**, the calculated ratios yielded values of 1.27 and 0.93, respectively. In other words, host protons H_a and H_b in complex **1a·3** have more intense intermolecular cross-peaks with the methylene than with the methyl group of **3**. For complex **1b·3**, the opposite is observed for the host H_a proton, while for the H_b proton, similar volumes are observed.

(20) Bothner-By, A. A.; Stephens, R. L.; Lee, J.-M. *J. Am. Chem. Soc.* **1984**, *106*, 811.

SCHEME 1[a] **Synthesis of Receptor 1**

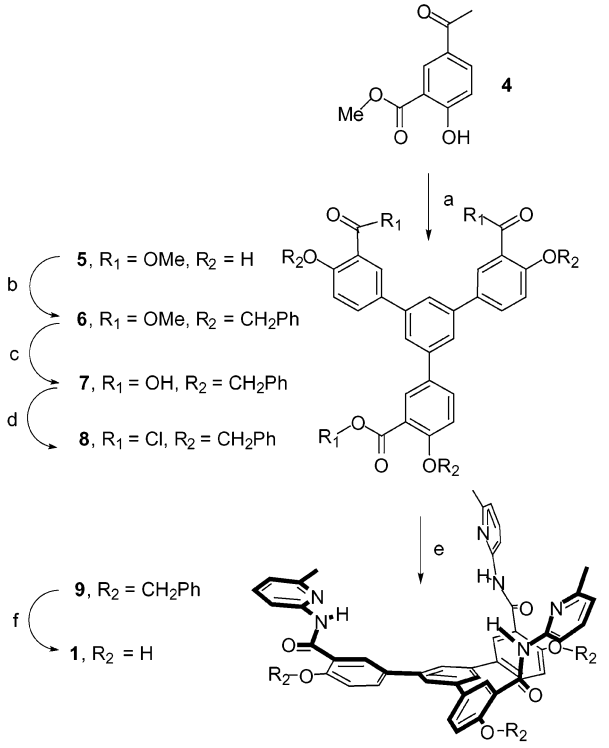

[a] Reagents and conditions: (a) $SiCl_4$/ EtOH, rt 14 h; (b) Cs_2CO_3, DMF/acetone, $BrCH_2Ph$, reflux, 24 h; (c) NaOH/THF, reflux, 20 h; HCl, 5%; (d) $SOCl_2/CH_2Cl_2$, reflux, 2 h; (e) 2-amino-6-methylpyridine, rt, 4 h; (f) Me_3SiI/CH_2Cl_2, rt, 72 h or $HBr/CHCl_3$, rt, 10 min.

Molecular modeling studies suggest two possible C_3-symmetric geometries for a complex between **3** and **1a** or **1b** in which six intermolecular hydrogen bonds between the three COOH residues of the triacid and the three CONH(py)N groups of the receptor can be established (Figure 4). In geometry **A**, the methyl group of **2** is endo to the receptor cavity, while in geometry **B**, it is exo. Both geometries were optimized with MacroModel 6.0[12] using the AMBER* force field and the GB/SA $CHCl_3$ solvation model, resulting in an energy difference of $\Delta E = \sim 3$ kcal/mol in favor of binding geometry **A** for the two complexes.

On the basis of the complexes obtained by molecular modeling, the **A** geometry (methyl group endo) should yield intermolecular contacts between the H_a and H_b protons on the receptor and the methyl and methylene protons of the triacid. Conversely, for the **B** geometry (methyl group exo), one should expect only intermolecular contacts between the above-mentioned receptor protons and the methylene proton of triacid **3**.

SCHEME 2[a] **Synthesis of Receptors 1a and 1b**

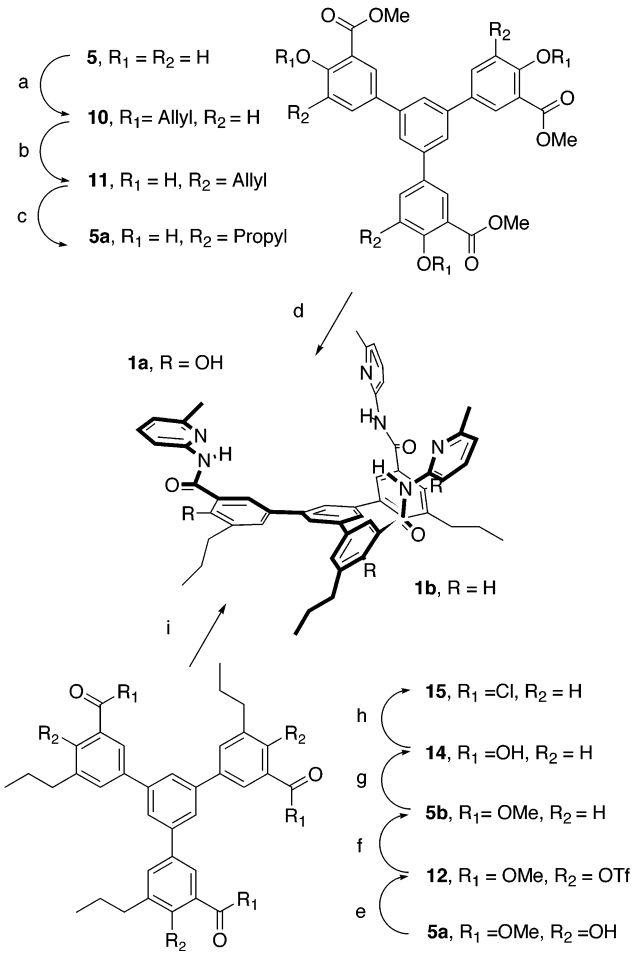

[a] Reagents and conditions: (a) Cs_2CO_3, DMF/acetone, $Br-CH_2-CH=CH_2$, reflux, 24 h; (b) *N*,*N*-dimethylaniline, reflux, 12 h; (c) H_2, 10% Pd/C, ethyl acetate, 10 psig, 5 h; (d) 4.5 equiv Me_3Al, then Me_3Al/2-amino-6-methylpyridine complex, benzene, reflux, 48 h; (e) Tf_2O, CH_2Cl_2; (f) $Cl_2Pd(PPh_3)_2$, Bu_3N, HCO_2H/DMF, 90 °C; (g) NaOH, H_2O/THF, then H^+; (h) $SOCl_2/CH_2Cl_2$; (i) 6-methyl-2-aminopyridine, CH_2Cl_2.

First, the observed ROEs between the methyl group of triacid **3** and the intracavity protons of the receptors provide strong experimental evidence for solution geometry **A**, but they do not rule out the presence of geometry **B** as well. Second, due to the considerably different H_a/H_b−methyl/methylene ROESY cross-peak volume ratios and the unequal chemical shift for the triacid methyl group for each complex, one can speculate on the existence of a solution equilibrium that involves different populations of geometries **A** and **B**. The relative amounts of the solution populations would be dictated by receptor structures that differ only on the phenolic OH. The interplay of intra- and intermolecular forces could be a possible cause for the different geometry populations.

VT ^{1}H NMR experiments were carried out in order to detect the existence of different complex geometries in solution. Lowering the temperature of the ^{1}H NMR experiment should slow the equilibration process, if one exists. If the temperature passes below the decoalescence point, the simultaneous observation of different ^{1}H NMR signals for the two complex geometries is possible. Figure 5 shows two VT ^{1}H NMR experiments, centered on the

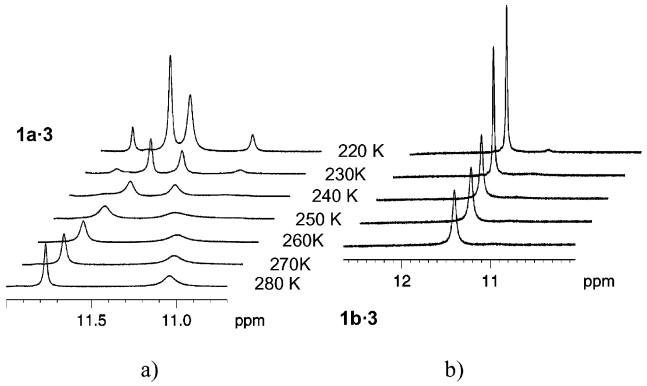

FIGURE 5. Downfield region of the VT ^{1}H NMR spectra for (a) complex **1a·3** and (b) complex **1b·3**.

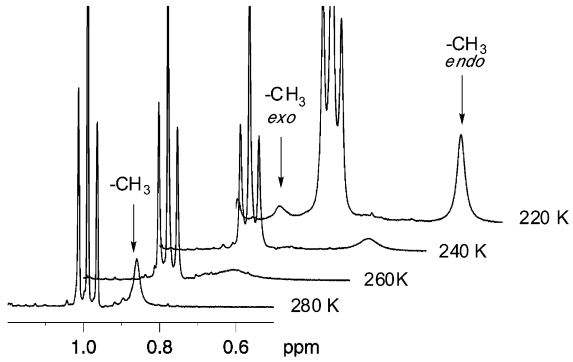

FIGURE 6. Upfield region of the VT ^{1}H NMR spectra for complex **1a·3**.

downfield region corresponding to the acidic protons (NH and phenolic OH of complex **1a·3**, NH of complex **1b·3**).

For complex **1a·3**, two sets of signals for each NH and OH proton are clearly seen at low temperature (230 K). These sets of signals had arisen through a decoalescence process from the two signals observed at room temperature and were assigned to the amide NH (∼10.98 ppm) and phenolic OH (∼11.79 ppm). Both sets of signals have chemical shifts that can be assigned to hydrogen-bonded protons. The observed temperature dependence of the system provides clear evidence for an equilibrium that becomes slow on the NMR time scale at around 240 K, allowing for the simultaneous observation of both of its components below that temperature. The relative population of the equilibrium components below decoalescence can be measured by integration of the signals of the different sets and was determined to be a 3:1 ratio at 220 K.

The remaining task was to determine the geometries of the major and minor components of the observed equilibrium. Close inspection of the region corresponding to the methyl group of triacid **3** in the VT ^{1}H NMR spectra revealed some important clues (Figure 6).

During the cooling process, the methyl group of **3**, which appeared initially as a singlet at 0.86 ppm, decoalescences into two signals clearly observable at 220 K. The major signal appears at 0.6 ppm, while the minor is at 1.2 ppm. In the endo geometry (**A**), the methyl group of **3** is directed toward the central aromatic ring of the receptor and is likely to experience an upfield shift under the influence of the magnetic anisotropy of the aromatic

ring, compared to the same methyl group in the exo geometry. Also, 1D NOE difference experiments carried out at 220 K reveal intense negative NOEs for the intracavity protons of the receptor upon irradiation at 0.6 ppm (upfield methyl signal of **3**). Thus, the major component of the equilibrium at 220 K can be assigned to the endo geometry (**A**) of complex **1a·3**, while the minor component can be assigned the exo geometry (**B**).

As for the room-temperature populations, the chemical shifts for the NH and the OH of the receptor and the methyl signal of **3** are much closer to the values ascribed to the minor geometry (i.e. exo) at 220 K. Furthermore, as discussed above, the room temperature 2D-ROESY experiment reveals more intense correlation peaks between the intracavity protons of the receptor (H_a, H_b) and the methylene signal of **3** than with the methyl signal of **3**. These observations suggest a change of the relative populations of the complex geometries from 220 K to room temperature, that is, an increase of the relative amount of the exo geometry upon warming. A likely explanation is that the temperature regulates the interplay between the inter- and intramolecular forces, which in turn controls the binding mode. The maximization of the intermolecular hydrogen bonds established in the endo geometry requires some conformational distortion and, therefore, a weakening of the intramolecular hydrogen bonds (vide infra). This maximization can only be achieved at low temperatures, where intermolecular hydrogen bonds become stronger due to the loss of vibrational motion in the complex. Analysis of the ^{1}H NMR signals of the hydrogen-bonded protons at 220 K (Figure 5a) provides further experimental support for this hypothesis. Indeed, the phenol proton for the major isomer (endo) is shifted upfield by 0.3 ppm relative to that of the minor isomer, a sign of weaker intramolecular hydrogen bonding. Furthermore, the amide proton for the major isomer is shifted downfield by 0.3 ppm compared to the same signal for the minor isomer, another sign of strengthened intermolecular hydrogen bonding.

Similar VT ^{1}H NMR experiments performed with complex **1b·3** gave a completely different picture. First of all, the amide NHs of **1b** do not show any sign of decoalescence in the same range of temperatures used for the study of complex **1a·3** (Figure 5b). The only temperature-dependent phenomenon observed for the amide NH protons of **1b** and the methyl group protons of **3** is a slight chemical shift change (downfield shift for the NH and upfield shift for the methyl), which can be simply ascribed to a tightening of the complex at lower temperature. These observations provide clear evidence for the nonexistence of equilibrating geometries for this host−guest system. Thus, for complex **1b·3**, one geometry is highly predominant in solution within a wide range of temperatures. Again, through 1D NOE difference experiments at 220 K and by comparing the chemical shift of the methyl group of **3** at that temperature to that of the endo geometry of complex **1a·3**, the geometry of complex **1b·3** was assigned to be almost exclusively endo.

The thermodynamic binding data for systems **1a·3** and **1b·3** were determined using isothermal titration calorimetry (ITC)[21] in a solvent mixture of 20% THF/$CHCl_3$. The host concentrations were adjusted to return a "*c*"[22] value approximately equal to 9, high enough for a reliable calorimetric determination of K_a and ΔH without compromising the solubility of the host and guest. Accordingly, hosts **1a** and **1b** were titrated by ITC as ≈1.5−2 mM solutions with a solution of **3** (12−17 mM), and the results are reported in Table 1. The enthalpy results clearly show that host **1b**, lacking the intramolecular hydrogen bond (phenolic hydroxyl to amide carbonyl), promotes more optimal H-bonding interactions with **3** than host **1a**. The conformational changes induced upon complexation in host **1a** reduce the exothermicity of association by ≈0.7 kcal/mol compared to **1b**, corresponding to the gain in energy due to the distortion of the intra- and intermolecular hydrogen-bonding networks of complex **1a·3**. The more flexible host **1b** can achieve better complementarity with **3** by maximizing the H-bonding interactions at the expense of a higher entropy loss.[23] The result is a lower value for its association constant.

TABLE 1. Isothermal Titration Calorimetry for Hosts 1a and 1b with 3 (MMTA) in 20% THF/$CHCl_3$, at 294 K

host	K_a (M^{-1})	ΔH (kcal/mol)
1a	10185 ± 350	−5.8 ± 0.2
1b	6690 ± 200	−6.5 ± 0.4

Attempts to obtain X-ray crystal structures for complexes **1a·3** and **1b·3** were successful. Slow diffusion of cyclohexane into 1:1 chloroform solutions of either **1a·3** or **1b·3** at room temperature produced colorless plates that were relatively unstable once removed from the mother liquor. For this reason, they were mounted on Lindeman capillaries prior to the dataset acquisition. Interestingly, the X-ray structure of complex **1a·3** reveals an unique host−guest geometry (Figure 7).

As expected, triacid **3** is docked into the receptor via six intermolecular hydrogen bonds. However, the structure shows a complex geometry that is related to the exo geometry proposed previously, based on the NMR data and modeling studies, except that it does not possess the idealized C_3-symmetry. Two of the guest carboxylic acids are almost coplanar with their respective amidopyridine binding unit, while the third acid is almost perpendicular to its amidopyridine partner. The O···N distances for the former NH···O interactions are shorter (2.8 Å) than for the latter (3.1 Å), while the O···N distances for the N···HO hydrogen bonds are the same for both types of hydrogen-bonded pairs (3.1 Å). The methyl group of the triacid does point away from the receptor cavity (exo). The dihedral angle about the amide−aryl planes is different for each arm (5°, 11°, and 13°). These values represent a distortion from the planarity required for the intramolecular phenolic hydrogen bond. The crystal data are in line with the hypothesis that, at room temperature, the exo/endo equilibrium for the geometries of complex **1a·3** is biased toward the exo geometry, since the latter is the adopted geometry for crystallization of the complex at room temperature. The lack of C_3-symmetry of the (**1a·3**)**A** structure may be attributed to packing preferences

(21) (a) Wadsö, I. *Chem. Soc. Rev.* **1997**, *26*, 79−86. (b) Freire, E.; Mayorga, O. L.; Straume, M. Anal. *Chem.* **1990**, *62*, 950−959. (c) Jelesarov, I.; Bosshard, H. R. *J. Mol. Recognit.* **1999**, *12*, 3−18.

(22) The "*c*" parameter ($c = K_a M_{tot} n$, M_{tot} = total host concentration, n = number of binding sites) should be between 5 and 500 for the accurate simultaneous determination of ΔH, K_a, and n. *Micro Calorimetry System User's Manual*, MicroCal ITC manual, pp 46−47.

(23) Searle, M. K.; Westwell, M. S.; Williams, D. H. *J. Chem. Soc., Perkin Trans. 2* **1995**, 141−151.

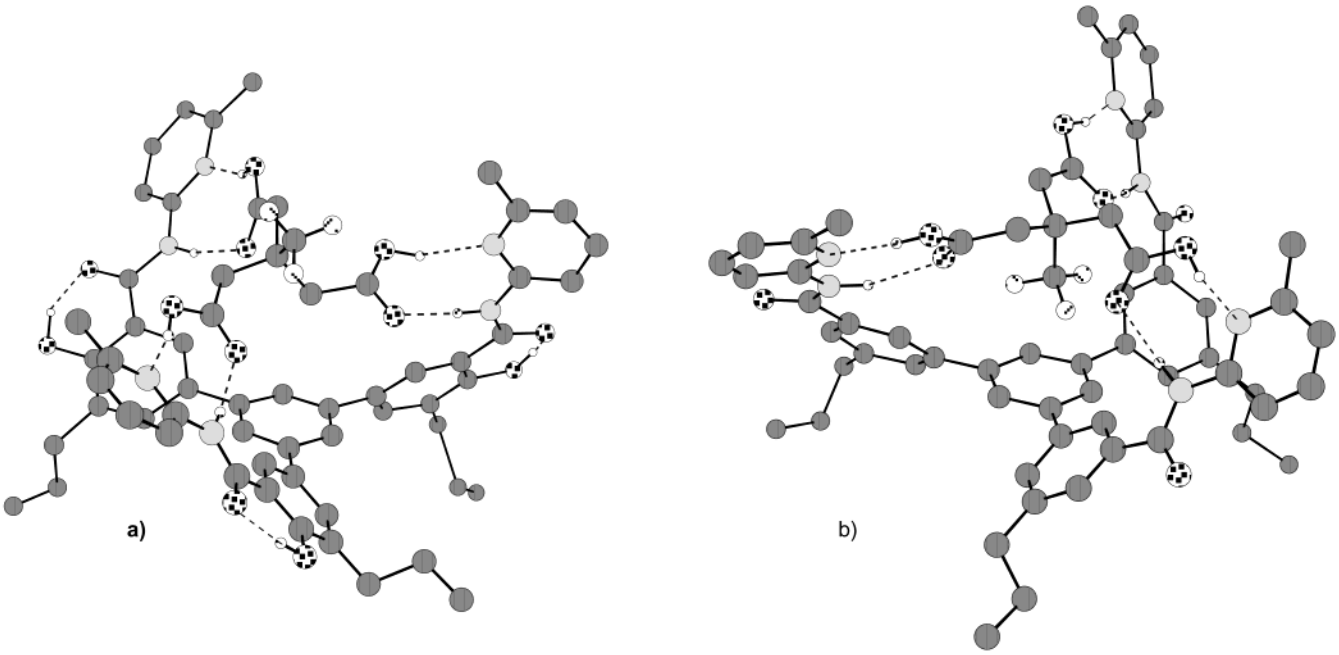

FIGURE 7. X-ray structures of (a) complex **1a·3** and (b) complex **1b·3**. Only polar hydrogens and MTA methyl hydrogens in calculated positions are shown. Dotted lines indicate inter- and intramolecular hydrogen bonds.

of the crystal and to the presence of disordered solvent molecules, as was previously observed in the crystal structure of complex **1a·2**.[8]

Gratifyingly, the X-ray structure of complex **1b·3** is in complete agreement with the endo structure proposed from solution analyses. It features a C_3-symmetry axis, and the methyl group of the triacid **3** points directly toward the interior of the receptor cavity, perpendicular to the central aromatic ring. Triacid **3** is docked into the receptor, establishing an array of six hydrogen bonds. Only two types of O···N distances for the six hydrogen-bonded interactions are observed, namely 2.6 Å and 2.9 Å for the NH···O and N···HO hydrogen bonds, respectively. The dihedral angle about the amide−aryl planes is 30° for all three arms. Since it is known that aromatic carboxamides prefer to remain coplanar to their aryl ring (conjugation), the observed tilt of the amides in complex **1b·3** provides a nice example of Koshland's induced-fit hypothesis in an abiotic setting.[9]

The observed amide-aryl dihedral angle in complex **1b·3** has the optimum value required for maximizing the intermolecular interactions in the endo geometry. This conformational condition cannot be achieved with receptor **1a** on binding triacid **3**. In receptor **1a**, the intramolecular hydrogen bonds between phenols and amide carbonyls restrict the rotation of the $C_{aryl}-C_{amide}$ bond and lock each amidopyridine subunit in an almost coplanar configuration with respect to their respective aryl ring. In complex **1a·3**, competition between intramolecular vs intermolecular hydrogen bonding results in only a partial tilt of the amides, such that the exo geometry arises as the preferred binding conformation instead of the endo geometry seen in complex **1b·3**.

Conclusion

We have reported the synthesis of several tripodal amidopyridine abiotic receptors that display high affinity for binding C_3-symmetric triacids, such as 1,3,5-cyclohexanetricarboxylic acid (**2**) and methylmethanetriacetic acid (**3**). We have studied the effect of remote intramolecular hydrogen bonding, used to restrict receptor conformation, on the binding mode of complex formation with triacid **3** and on the thermodynamic parameters of the binding process. Molecular modeling studies suggest two possible C_3-symmetric geometries for a complex between **3** and **1a** or **1b** in which six intermolecular hydrogen bonds between the triacid guest and the receptor can be established. VT ^{1}H NMR experiments, as well as 1D and 2D NOE experiments, were carried out to ascertain the existence of an equilibrium between complex geometries and to map out their structural features. While the conformationally restricted receptor **1a** shows that its preferred binding geometry is temperature dependent, receptor **1b** binds **3** in a fixed geometry at any temperature. This difference in binding behavior was explained in terms of an interplay between intermolecular and intramolecular interactions. The binding processes have been studied by ITC, and again, an important influence of the remote intramolecular hydrogen bonding on the thermodynamics of binding was observed. Crystal structures of complexes **1a·3** and **1b·3** were obtained by X-ray crystallography. Each complex has a different binding geometry in the solid state that is in agreement with its predominant solution structure at room temperature (complex **1a·3** has exo geometry, while complex **1b·3** has preference for the endo mode). The geometrical parameters derived from the X-ray data clearly support a balance between intermolecular and intramolecular hydrogen-bonding interactions that is responsible for the different binding modes. On one hand, the remote intramolecular hydrogen bonds present in **1a** and ring conjugation of the carboxamide promote coplanarity of the amide and aryl planes. On the other hand, maximization of the intermolecular interactions with the more

flexible receptor **1b** forces a tilting of the amides away from coplanarity. The geometrical requirements of the intramolecular hydrogen bonds in **1a** force a change in binding mode in order to maximize the intermolecular interactions. Only at low temperatures is the energy gain of the strengthened intramolecular interactions capable of overcoming the loss of stability due to the distorted intramolecular interactions required to achieve optimal endo geometry. This model system shows how subtle effects, acting far away from the binding site, and temperature changes can switch the preferred binding geometry of a host−guest complex. Indeed, the interplay of inter- and intramolecular interactions should always be taken into consideration whenever predictions of binding modes are made.

Experimental Section

General Methods and Materials. Instrumentation. All reactions were run under argon in oven-dried glassware. ^{1}H (300 MHz) and ^{13}C NMR (75 MHz) spectra were recorded in $CDCl_3$ solutions. Chemical shifts (δ) are reported in ppm and referenced to the solvent peak.[24] Melting points were taken on a capillary melting point apparatus and are uncorrected. High-resolution mass spectra were obtained by electron impact ionization with an energy of 70 eV. Elemental analyses were performed by Servei de Microànalisi Elemental del Centre d'Investigació i Desenvolupament C. S. I. C. (Barcelona, Spain).

Materials. Preparative flash chromatography was performed on Merck silica gel 60 (40−63 mM). Analytical TLC was performed on precoated Merck silica gel 60 F-254 plates. Preparative TLC was performed on 0.5 mm precoated Scharlau silica gel SiF-254 Glasschrom plates.

Compounds. All commercially available compounds (Aldrich) were used without further purification unless otherwise indicated. Tetrahydrofuran (THF), toluene, benzene, and diethyl ether were distilled from sodium benzophenone ketyl. Ethyl alcohol and dichloromethane were distilled from calcium hydride. Acetone was distilled from K_2CO_3. *N*,*N*-Dimethylformamide (DMF) was dried over activated 4 Å molecular sieves.

Synthesis. Methyl 5-Acetyl-2-hydroxybenzoate (4). An oven-dried 500-mL, three-neck round-bottom flask, equipped with a mechanical stirrer, a thermometer, and a reflux condenser fitted with an argon inlet, was charged with 200 g of polyphosphoric acid (PPA). The flask was immersed in an oil bath heated at 80 °C and stirred. When the PPA temperature reached 80 °C, 12.2 mL (213 mmol) of glacial acetic acid was added at once. After 15 min, 25 mL of methyl salicylate was added at once and the reaction mixture stirred at this temperature for 2 h. The reaction mixture had turned dark and was poured over 1500 g of an ice−water mixture to hydrolyze the PPA. The resulting aqueous mixture was extracted with CH_2Cl_2 (5 × 100 mL). The organic extracts were combined, washed with 5% $NaHCO_3$ aqueous solution and brine, dried over Na_2SO_4, and concentrated by rotary evaporation to yield a dark red oil. The oil was vacuum distilled (0.1 mmHg), yielding a fraction of unreacted methyl salicylate collected between 60 and 70 °C and 7.7 g of **4** (20%) collected between 115 and 120 °C as a colorless thick liquid which turned to a white solid on standing: mp 59−61 °C; IR (KBr) 3300−3600 (broad), 1680, 1200, 1360 cm^{-1}; ^{1}H NMR ($CDCl_3$) δ 11.24 (s, 1H), 8.48 (d, J = 2.1 Hz, 1H), 8.09 (dd, J = 8.7, 2.1 Hz, 1H), 7.04 (d, J = 8.7 Hz, 1H), 4.00 (s, 3H), 2.58 (s, 3H); ^{13}C NMR ($CDCl_3$) δ 196.33, 170.62, 165.74, 135.96, 131.91, 129.49, 118.46, 112.50, 53.24, 26.80. An analytical sample of **4** was prepared by recrystallization from cyclohexane. Anal. Calcd for $C_{10}H_{10}O_4$: C, 61.85, H, 5.19. Found: C, 61.85, H, 5.23.

1,3,5-(4-Hydroxy-3-methoxycarbonylphenyl)benzene (5). A 500-mL three-neck round-bottom flask equipped with an argon inlet, a reflux condenser, a rubber septum and a magnetic stir bar was charged with 13.5 g (69.6 mmol) of ester **4** and 275 mL of dry ethanol. To the resulting solution, 48 mL (419 mmol) of $SiCl_4$ were slowly transferred via cannula. During the transfer, the reaction temperature rose to solvent reflux and a strong evolution of HCl was observed. The resulting wine red mixture was allowed to stir at room temperature for 15 h. then poured into 200 mL of ice water. A pink solid precipitated and was filtered on a fritted filter funnel. The collected pink solid was dissolved in CH_2Cl_2 and the resulting solution was dried over Na_2SO_4, filtered and concentrated by rotary evaporation to afford a solid residue that was washed with a small amount of diethyl ether to yield 10.7 g (87%) of pure triester **5** as a white solid: mp 222−225 °C; IR (KBr) 3300−3600 (broad), 1670, 1210, 1290 cm^{-1}; ^{1}H NMR ($CDCl_3$) δ 10.83 (s, 3H), 8.14 (d, J = 2.4 Hz, 3H), 7.81 (dd, J = 8.4, 2.4 Hz, 3H), 7.63 (s, 3H), 7.12 (d, J = 8.4 Hz, 3H), 4.00 (s, 9H); ^{13}C NMR ($CDCl_3$) δ 171.13, 161.9, 141.9, 135.3, 132.8, 129.0, 124.7, 118.8, 113.2, 53.1. An analytical sample of **5** was prepared by recrystallization from benzene. Anal. Calcd for $C_{30}H_{24}O_9$: C, 68.18, H, 4.58. Found: C, 68.15, H, 4.67.

Route to 1,3,5-Tris[3-(*N*-(6-methyl-2-pyridyl)carbamoyl-4-hydroxyphenyl]benzene (1). 1,3,5-(4-Benzyloxy-3-methoxycarbonylphenyl)benzene (6). A 500-mL three-neck round-bottom flask equipped with a magnetic stir bar, a rubber septum, and a reflux condenser fitted with an argon inlet adaptor was charged with 3.91 g (7.4 mmol) of triester **5**, 120 mL of dry acetone, and 75 mL of DMF. Benzyl bromide (3.6 mL, 33.3 mmol) was added by syringe, followed by 14.8 g (45.4 mmol) of Cs_2CO_3. The dark brown solution was refluxed for 14 h, allowed to cool to room temperature, filtered over Celite, and concentrated by rotary evaporation to afford a brown thick paste.[25] The paste was dissolved in 50 mL of diethyl ether and extracted with water (3 × 40 mL). The organic phase was dried over Na_2SO_4, filtered, and concentrated to yield the benzylated triester (5.3 g, 90%) as a light yellow solid: mp 176−178 °C; IR (KBr) 1730, 1690, 1610, 1500, 1450, 1260, 1090, 900 cm^{-1}; ^{1}H NMR ($CDCl_3$) δ 8.14 (d, J = 2.4 Hz, 3H), 7.74 (dd, J = 8.7, 2.4 Hz, 3H), 7.67 (s, 3H), 7.42 (m, 15H), 7.12 (d, J = 8.7 Hz, 3H), 5.26 (s, 6H), 3.95 (s, 9H); ^{13}C NMR ($CDCl_3$) δ 167.3, 158.4, 141.7, 137.3, 134.0, 132.7, 131.1, 129.2, 128.5, 127.5, 124.8, 121.7, 114.2, 71.3, 52.8. An analytical sample was prepared by recrystallization from ethyl acetate. Anal. Calcd for $C_{51}H_{42}O_9$: C, 76.68, H, 5.30. Found: C, 76.49, H, 5.40.

1,3,5-Tris(4-benzyloxy-3-carboxyphenyl)benzene (7). In a 250-mL round-bottom flask equipped with a magnetic stir bar and a reflux condenser fitted with an argon inlet were placed 4.7 g (5.9 mmol) of the benzylated triester prepared above and 150 mL of THF. To the resulting solution was added 150 mL of 3 N NaOH, and the mixture was refluxed under argon atmosphere for 20 h. A yellowish solid was collected after having removed most of the THF under reduced pressure. The solid was suspended in 50 mL of 5% HCl, stirred for 15 min, collected again, and dissolved in $CHCl_3$. The organic solution was dried over Na_2SO_4, filtered, and evaporated to afford triacid **6** (4.3 g, 6%) as a white solid: mp 130−132 °C. IR (KBr) 3300−3500 (broad), 1720, 1680, 1600, 1490, 1380, 1230 cm^{-1}; ^{1}H NMR ($CDCl_3$) δ 8.41 (d, J = 2.1 Hz, 3H), 7.85 (dd, J = 8.7, 2.1 Hz, 3H), 7.65 (s, 3H), 7.45 (m, 15H), 7.24 (d, J = 8.7 Hz), 5.35 (s, 6H); ^{13}C NMR ($CDCl_3$) δ 166.8, 157.8, 140.7, 135.2, 134.8, 134.1, 132.3, 129.7, 129.6, 128.6, 124.6, 118.8, 114.4,

(24) Reference values were taken from the Bruker Almanac 1992, as indicated in the tables of Properties of Some Important Solvents.

(25) ^{1}H NMR spectroscopy of an aliquot of the crude mixture reveals the presence of a significant amount of DMF. The following water extraction greatly reduces the amount of DMF.

72.8. Anal. Calcd for $C_{49}H_{36}O_9$: C, 76.18, H, 4.79. Found: C, 76.15, H, 4.76.

1,3,5-Tris(4-benzyloxy-3-chloroformylphenyl)benzene (8). 1,3,5-Tris(4-benzyloxy-3-carboxyphenyl)benzene (3.95 g, 5 mmol) was dissolved in a mixture of 30 mL of CH_2Cl_2 and 11.4 mL (156.7 mmol) of $SOCl_2$. The resulting clear solution was refluxed for 2 h. The solvent was evaporated in vacuo, affording a light brown solid of the triacid chloride (3.9 g, 87%), which was used in the next step without further purification: IR (KBr) 1770, 1730, 1600, 1490, 1290, 1260, 900 cm^{-1}; ^1H NMR ($CDCl_3$) δ 8.36 (d, $J = 2.3$ Hz, 3H), 7.85 (dd, $J = 8.7$, 2.3 Hz, 3H), 7.66 (s, 3H), 7.42 (m, 15H), 7.17 (d, $J = 8.7$ Hz, 3H), 5.29 (s, 6H); ^{13}C NMR ($CDCl_3$) δ 164.3, 158.9, 141.3, 136.3, 135.2, 133.8, 133.6, 129.3, 128.7, 127.4, 124.9, 123.5, 114.7, 71.3.

1,3,5-Tris[4-benzyloxy-3-(*N*-(6-methyl-2-pyridyl)carbamoyl)phenyl]benzene (9). In an oven-dried 250-mL, three-neck round-bottom flask equipped with a magnetic stir bar, a stopper, a rubber septum, and an argon inlet adaptor were placed 3.9 g (4.8 mmol) of the triacyl chloride prepared above and 100 mL of dry CH_2Cl_2. 2-Amino-6-methylpyridine (3.12 g, 28.8 mmol) was added in one portion and the resulting solution was stirred at room temperature for 4 h. The solution was diluted with 50 mL of CH_2Cl_2 and washed with 5% HCl (4×50 mL), 5% $NaHCO_3$, and brine, dried over Na_2SO_4, filtered, and concentrated in vacuo to afford the title compound (3.9 g, 78%) as a white solid: mp 223−225 °C; IR (KBr) 3450, 1660, 1530, 1450, 1300, 800, 740 cm^{-1}; ^1H NMR ($CDCl_3$) δ 10.44 (s, 3H), 8.62 (s, $J = 2.4$ Hz, 3H), 8.22 (d, $J = 8.4$ Hz, 3H), 7.82 (dd, $J = 8.7$, 2.4 Hz, 3H), 7.80 (s, 3H), 7.60 (m, 9H), 7.40 (m, 9H), 7.20 (d, $J = 8.7$ Hz, 3H), 6.86 (d, $J = 7.5$ Hz, 3H), 5.36 (s, 6H), 2.40 (s, 9H); ^{13}C NMR ($CDCl_3$) δ 163.9, 157.5, 156.9, 151.9, 141.4, 138.9, 135.9, 134.9, 132.7, 131.7, 129.4, 129.1, 128.5, 124.8, 122.8, 119.5, 114.2, 111.9, 72.3, 24.7. Anal. Calcd for $C_{66}H_{54}N_6O_6$: C, 77.17, H, 5.30, N, 8.18. Found: C, 77.15, H, 5.36, N, 8.20.

1,3,5-Tris[3-(*N*-(6-methyl-2-pyridyl)carbamoyl-4-hydroxyphenyl]benzene (1). Method A. In a 10-mL round-bottom flask equipped with a magnetic stir bar and a rubber septum was dissolved under argon atmosphere 100 mg (0.097 mmol) of the benzylated triamide prepared above in 2.5 mL of dry CH_2Cl_2. Iodotrimethylsilane (206 mL, 1.455 mmol) was added to the above solution by syringe and the reaction mixture was stirred for 72 h. MeOH (2 mL) was added and the reaction stirred further for 5 min. The solvent was evaporated in vacuo to afford a dark brown solid. Trituration of the solid with several 5 mL portions of diethyl ether yielded 62 mg (85%) of the triamide **1** as a brown solid.

Method B. HBr gas was bubbled for 5−10 min into a solution of 250 mg (0.243 mmol) of the benzylated triamide prepared above in 15 mL of $CHCl_3$. A yellowish precipitate was formed, then 10 mL of 5% $NaHSO_4$ followed by 20 mL of THF was added, and the mixture was stirred for 20 min. When all the solids had completely dissolved, the organic layer was separated, washed with brine, dried over Na_2SO_4, filtered, and evaporated in vacuo to afford a solid. Trituration of the solid with several portions of hexanes yielded 184 mg of pure triamide **1** (58%) which was dried on a drying pistol under vacuum over P_2O_5 using refluxing ethyl acetate: mp >300 °C; IR (KBr) 3400−3500 (broad), 1640, 1570, 1300, 1170, 800 cm^{-1}; ^1H NMR (DMSO-d_6) δ 12.3 (s, 3H), 11.07 (s, 3H), 8.58 (s, 3H), 8.18 (d, $J = 8.1$ Hz, 3H), 8.10 (d, $J = 8.1$ Hz, 3H), 8.00 (s, 3H), 7.85 (t, $J = 7.8$ Hz, 3H), 7.30 (d, $J = 8.1$ Hz, 3H), 7.14 (d, $J = 7.5$ Hz, 3H), 2.54 (s, 9H); ^{13}C NMR (DMSO-d_6) δ 170.5, 162.9, 162.7, 156.6, 146.6, 144.5, 140.3, 138.5, 137.5, 134.5, 128.9, 125.1, 123.8, 117.2, 29.5.

Route to 1,3,5-Tris(3-(*N*-6-methyl-2-pyridyl)carbamoyl-4-hydroxy-5-propylphenyl)benzene (1a). 1,3,5-Tris-(4-allyloxy-3-methoxycarbonylphenyl)benzene (10). In an oven-dried 1-L three-neck round-bottom flask equipped with an argon inlet adaptor, a magnetic stirring bar, a reflux condenser, and a rubber septum were dissolved 10.7 g (20.3 mmol) of the triester **5** with 300 mL of freshly distilled dry acetone and 275 mL of dry DMF. Next, 7.9 mL (91.3 mmol, $d = 1.398$ g/mL) of allyl bromide was added to the solution by syringe. After several minutes, 39.7 g (121.8 mmol) of Cs_2CO_3 was added, producing a change of the solution's color from pink to brown dark. The mixture was stirred and refluxed under argon during 14 h. The reaction mixture was allowed to reach room temperature and filtered through Celite. The filtered solution was concentrated by rotary evaporation to yield a brown sticky solid. The solid was dissolved in 50 mL of diethyl ether and extracted with water (3×40 mL). The organic phase was dried over Na_2SO_4, filtered, and concentrated to yield 1,3,5-tris(4-allyoxy-3-methoxycarbonylphenyl)benzene (11.2 g, 85%) as a brown solid: mp 56−60 °C; IR (KBr) 1720, 1600, 1500, 1260, 850 cm^{-1}; ^1H NMR ($CDCl_3$) δ 8.12 (d, $J = 2.5$ Hz, 3H), 7.76 (dd, $J = 8.7$, 2.5 Hz, 3H), 7.67 (s, 3H), 7.07 (d, $J = 8$ Hz, 3H), 6.10 (ddt, $J = 17.2$, 10.6, 4.7 Hz, 3H) 5.55 (ddt, $J = 17.2$, 1.5, 1.5 Hz, 3H), 5.34 (ddt, $J = 10.6$, 1.5, 1.3 Hz, 3H), 4.70 (ddd, $J = 4.7$, 1.5, 1.3 Hz, 6H); ^{13}C NMR ($CDCl_3$) δ 167.35, 158.39, 141.68, 133.81, 133.27, 132.70, 131.09, 124.79, 121.47, 118.22, 114.68, 70.22, 52.84.

An analytical sample was prepared by recrystallization from CH_2Cl_2/MeOH. Anal. Calcd for $C_{39}H_{36}O_9$: C, 72.21, H, 5.59. Found: C, 72.17, H, 5.60.

1,3,5-Tris(5-allyl-4-hydroxy-3-methoxycarbonylphenyl)-benzene (11). In a dry 100-mL round-bottom flask equipped with magnetic stir bar and reflux condenser was dissolved 10 g (15.4 mmol) of the above prepared triester in 20 mL of *N*,*N*-dimethylaniline freshly distilled under vacuum. The reaction mixture was refluxed under argon atmosphere during 13 h. The reaction mixture was allowed to cool and was diluted with 100 mL of diethyl ether. The organic solution was extracted with 5% HCl (3×50 mL) and brine (50 mL), dried over Na_2SO_4, filtered, and evaporated to dryness, affording 9 g (90%) of the title compound as a brown solid: mp 199−202 °C; IR (KBr) 3300−3600 (broad), 1670, 1440, 800 cm^{-1}; ^1H NMR ($CDCl_3$) δ 11.12 (s, 3H), 8.02 (d, $J = 2.4$ Hz, 3H), 7.64 (d, $J = 2.4$ Hz, 3H), 7.59 (s, 3H), 6.07 (ddt, $J = 2.4$, 10.2, 6.5 Hz, 3H), 5.13 (m, 6H), 3.98 (s, 9H), 3.53 (d, $J = 6.5$ Hz, 6H); ^{13}C NMR ($CDCl_3$) δ 171.53, 159.98, 142.25, 136.67, 135.46, 132.54, 129.93, 127.18, 124.90, 116.88, 112.65, 53.11, 34.58.

1,3,5-Tris(4-hydroxy-3-methoxycarbonyl-5-propylphenyl)benzene (5a). In a 250-mL Parr shaker hydrogenation flask, 900 mg of Pd/C 10% was suspended in a solution prepared by mixing 9 g (13.9 mmol) of the triester above in the minimum amount of ethyl acetate. The suspension was shaken for 2 h at room temperature with 9 psig of H_2. The catalyst was filtered through Celite and the solvent was evaporated in vacuo, yielding 8.4 g (92%) of **5a** as a white solid: mp 212−215 °C; IR (KBr) 3400 (broad), 3150 (broad), 1676, 1440, 1240, 1200, 1140, 800 cm^{-1}; ^1H NMR ($CDCl_3$) δ 11.10 (s, 3H), 8.02 (d, $J = 2.1$ Hz, 3H), 7.66 (d, $J = 2.1$ Hz, 3H), 7.62 (s, 3H), 3.98 (s, 9H), 2.75 (t, $J = 7.5$ Hz, 6H), 1.73 (m, 6H), 1.02 (t, $J = 7.3$ Hz, 9H); ^{13}C NMR ($CDCl_3$) δ 171.70, 160.26, 142.36, 135.52, 132.40, 132.33, 126.71, 124.82, 112.68, 53.09, 32.70, 23.45, 14.75. Anal. Calcd for $C_{39}H_{42}O_2$: C, 71.54, H, 6.47. Found: C, 71.60, H, 6.46.

1,3,5-Tris(3-(*N*-6-methyl-2-pyridyl)carbamoyl-4-hydroxy-5-propylphenyl)benzene (1a). An oven-dried 250-mL three-neck round-bottom flask equipped with a magnetic stir bar, a glass stopper, and a rubber septum was charged with 4 g (6.1 mmol) of triester **5a** and 50 mL of freshly distilled dry benzene under argon. The resulting suspension was cooled at 0 °C with an ice bath, and 13.8 mL (27.5 mmol) of 2 M $AlMe_3$ was slowly transferred via cannula, maintaining the reaction mixture temperature at 0 °C throughout the addition. The reaction mixture was stirred at room temperature for 20 min. Using a similar procedure, 2.98 g (27.5 mmol) of 2-amino-6-methylpyridine dissolved in 50 mL of benzene was treated with 13.8 mL (27.5 mmol) of 2 M $AlMe_3$. The amine solution was added via cannula to the ester solution and the reaction mixture was heated to reflux for 48 h. During this time, a brownish

precipitate appeared in the mixture. The reaction mixture was poured over 50 g of ice and 2 M HCl was added until the pH of the aqueous layer was approximately 4−5. The aqueous layer was extracted with $CHCl_3$ (4 × 40 mL). The combined organic extracts were washed with 5% $NaHSO_4$ (2 × 60 mL) and brine (50 mL) and dried over Na_2SO_4, and the solvent was removed by rotary evaporation, yielding a solid. ^{1}H NMR analysis of the solid revealed a complex mixture. Flash chromatography of the solid using CH_2Cl_2/EtOAc (98:2) afforded three different fractions: starting material, monoamide diester, and diamide monoester. The triamide was eluted using CH_2Cl_2/EtOAc (90:10), and rotary evaporation of the solvent yielded 1.4 g (25.9%) of **1a** as a pale yellow solid: mp 281−285 °C. IR (KBr) 3200−3500 (broad), 1640, 1540, 1450, 1310, 790 cm^{-1}; ^{1}H NMR ($CDCl_3$) δ 12.19 (s, 3H), 8.93 (s, 3H), 8.09 (d, J = 8.1 Hz, 3H), 7.78 (s, 3H), 7.62 (m, 9H), 6.90 (d, J = 7.2 Hz, 3H), 2.77 (t, J = 7.6 Hz, 6H), 2.34 (s, 9H), 1.76 (m, 6H), 1.04 (t, J = 7.2 Hz, 9H); ^{13}C NMR ($CDCl_3$) δ 169.88, 160.77, 157.46, 150.92, 141.72, 139.29, 134.20, 133.39, 131.56, 123.85, 123.03, 120.28, 114.50, 112.18, 32.84, 24.21, 23.42, 14.89.

An analytical sample was prepared by recrystallization from benzene. Anal. Calcd for $C_{54}H_{54}N_6O_6$: C, 73.45, H, 6.16, N, 9.52. Found: C, 73.50, H, 6.18, N, 9.54.

Route to 1,3,5-Tris[3-(*N*-6-methyl-2-pyridyl)carbamoyl-5-propylphenyl]benzene (1b). 1,3,5-Tris(3-methoxycarbonyl-5-propyl-4-trifluoromethanesulfonyphenyl)-benzene (12). A 100-mL round-bottom flask equipped with a magnetic stir bar, a rubber septum, and an argon inlet was charged with 1 g (1.53 mmol) of triester **5a** and 20 mL of anhydrous pyridine. The resulting suspension was slightly heated to induce complete solution of the triester. The solution was cooled in an ice bath and 1.5 mL (d = 1.719 g/mL, 9.14 mmol) of triflic anhydride was added by syringe. During the addition, the temperature rose and the color of the solution turned intense violet. The reaction mixture was stirred during 3 days at room temperature. The reaction mixture was diluted with 50 mL of CH_2Cl_2 and washed with 5% HCl (5 × 20 mL), an aqueous solution of $CuSO_4$ (until persistence of the blue color), and water. The organic phase was dried over Na_2SO_4, filtered, and evaporated to dryness, affording an amber solid that was purified by percolation on silica gel using 100 mL of CH_2Cl_2. Rotary evaporation of the solvent yields 1.25 g (78%) of the title compound as a white solid: mp 153−155 °C; ^{1}H NMR ($CDCl_3$) δ 8.097 (d, J = 2.43 Hz, 3H), 7.762 (s, 3H), 7.750 (s, 3H), 3.983 (s, 3H), 2.837 (t, J = 7.71 Hz, 6H), 1.768 (m, 6H), 1.033 (t, J = 7.26 Hz, 9H); ^{13}C NMR ($CDCl_3$) δ 165.13, 145.12, 140.56, 140.16, 137.51, 133.44, 128.79, 126.21, 126.09, 118.55 (q), 52.81, 32.06, 23.42, 13.81.

An analytical sample was prepared by recrystallization from ethanol. HRMS calcd for $C_{42}H_{39}F_9O_{15}S_3$ 1050.1307, found 1050.1309.

1,3,5-Tris(3-methoxycarbonyl-5-propylphenyl)benzene (5b). A 50-mL three-neck round-bottom flask equipped with stir bar, reflux condenser, and argon inlet adaptor was charged with 1 g (0.95 mmol) of the triflate prepared above and 19 mL of anhydrous DMF. To the resulting solution were successively added 0.163 g (0.23 mmol) of $PdCl_2(PPh_3)_3$, 0.22 g (0.55 mmol) of 1,3-bisdiphenylphosphinopropane, 3.75 mL (15.74 mmol) of triethylamine, and 0.38 mL (10.07 mmol) of formic acid. The color of the solution turned brown dark. The reaction mixture was stirred for 9 h at 110 °C under argon. The reaction mixture was diluted with 50 mL of CH_2Cl_2 and washed with 5% HCl (3 × 15 mL), 5% $NaHCO_3$ (3 × 15 mL), and brine (3 × 15 mL). The organic layer was dried over Na_2SO_4, filtered, and concentrated under vacuum. The crude product was purified by column chromatography on silica gel (CH_2Cl_2) to give 0.810 g (81%) of the title compound as a white solid: mp 144−147 °C; ^{1}H NMR ($CDCl_3$) δ 8.186 (s, 3H), 7.908 (s, 3H), 7.796 (s, 3H), 7.694 (s, 3H), 3.957 (s, 9H), 2.744 (t, J = 7.62 Hz, 6H), 1.739 (m, 6H), 0.992 (t, J = 7.2 Hz, 9H); ^{13}C NMR ($CDCl_3$) δ 167.21, 143.72, 141.83, 141.15, 132.14, 130.71, 128.81, 125.98, 125.58, 52.17, 37.86, 24.54, 13.78.

An analytical sample was prepared by recrystallization from ethanol. Anal. Calcd for $C_{39}H_{42}O_6$: C, 77.20, H, 6.98. Found: C, 77.25, H, 7.00.

1,3,5-Tris(3-carboxy-5-propylphenyl)benzene (14). A 250-mL one-neck round-bottom flask was charged with 0.8 g (1.32 mmol) of the triester prepared above, 57 mL of THF, and 57 mL of 3 N NaOH. The reaction mixture was refluxed overnight. Then the THF was eliminated by rotary evaporation. The aqueous layer was washed three times with 20 mL of diethyl ether and acidified by slow addition of concentrated HCl, affording a white solid. The solid was taken up in a solvent mixture THF/Et_2O (3:7). The organic phase was dried over Na_2SO_4, filtered, and evaporated to dryness, yielding 0.62 g (83.3%) of the title product as a white solid: mp 260 °C dec; IR (KBr) 3000 (broad), 1692, 1599, 1450, 1300, 731 cm^{-1}; ^{1}H NMR (DMSO-d_6) δ 13.105 (s, 3H), 8.233 (s, 3H) 8.044 (s, 3H), 8.018 (s, 3H), 7.920 (s, 3H). 2.839 (t, J = 7.2 Hz, 6H), 1.784 (m, 6H), 1.038 (t, J = 7.2 Hz, 9H); ^{13}C NMR (DMSO-d_6) δ 171.35, 147.47, 145.25, 144.34, 135.91, 135.43, 132.43, 129.42, 129.06, 40.92, 28.06, 17.60.

Anal. Calcd for $C_{36}H_{36}O_6$: C, 76.57, H, 6.43. Found: C, 76.50, H, 6.49.

1,3,5-Tris(3-chloroformyl-5-propylphenyl)benzene (15). The triacid (0.620 g, 1.1 mmol) prepared above was suspended in 15 mL of $SOCl_2$. The suspension was refluxed for 2 h, and the solvent was evaporated to dryness, affording a light brown solid. Trituration of the solid with hexane gave 0.654 g (99.8%) of the triacyl chloride, which was used in the next step without further purification: ^{1}H NMR ($CDCl_3$) δ 8.36 (d, J = 2.3 Hz, 3H), 7.85 (dd, J = 8.7, 2.3 Hz, 3H), 7.66 (s, 3H), 7.42 (m, 15H), 7.17 (d, J = 8.7 Hz, 3H), 5.29 (s, 6H); ^{13}C NMR ($CDCl_3$) δ 164.3, 158.9, 141.3, 136.3, 135.2, 133.8, 133.6, 129.3, 128.7, 127.4, 124.9, 123.5, 114.7, 71.3.

1,3,5-Tris[3-(*N*-6-methyl-2-pyridyl)carbamoyl-5-propylphenyl]benzene (1b). A 50-mL, one-neck round-bottom flask equipped with a magnetic stir bar and an argon inlet was charged with 654 mg (1.1 mmol) of the triacyl chloride prepared above and 20 mL of dry CH_2Cl_2. 2-Amino-6-methylpyridine (1.1 g, 10.2 mmol) was added in one portion and the resulting solution was stirred at room temperature for 4 h. The solution was diluted with 20 mL of CH_2Cl_2, washed with 5% HCl (4 × 50 mL), 5% $NaHCO_3$, and brine, dried over Na_2SO_4, filtered, and evaporated in vacuo. The residue was purified by column chromatography (CH_2Cl_2/hexane/THF, 78:20:2) to furnish 664 mg (72.6%) of **1b** as a white solid: mp 178−180 °C; MS: m/z 835 (24.5%, M$^+$), 739 (100%); ^{1}H NMR ($CDCl_3$) δ 8.67 (s, 3H), 8.22 (d, J = 8.3 Hz, 3H), 8.08 (t, J = 1.5 Hz), 7.86 (s, 3H), 7.77 (t, J = 1.5 Hz, 3H), 7.72 (t, J = 1.5 Hz, 3H), 7.65 (t, J = 7.7, 3H), 6.93 (d, J = 7.5, 3H), 2.773 (t, J = 7.2 Hz, 6H), 2.452 (s, 9H), 1.76 (m, 6H), 1.01 (t, J = 7.2 Hz, 9H); ^{13}C NMR ($CDCl_3$) δ 166.1, 157.3, 151.3, 144.7, 142.2, 141.9, 139.2, 135.5, 131.8, 126.9, 126.2, 124.2, 119.8, 111.4, 38.4, 25.0, 24.4, 14.3. Anal. Calcd for $C_{54}H_{54}N_6O_3$: C, 77.67, H, 6.52, N, 10.06. Found: C, 77.65, H, 6.46, N, 10.10.

Acknowledgment. We thank the DGESIC (Projects PB 98-0129 and SAB 1998-0109) for financial support and the sabbatical leave of Prof. Deslongchamps, respectively.

Supporting Information Available: Crystal data (CIF) for complexes **1a·3** and **1b·3**. This material is available free of charge via the Internet at http://pubs.acs.org.

JO025787L